



Short communication

## Fabrication of a high-performance Pb–PtCu/CNT catalyst for methanol electro-oxidation

Yiyin Huang, Jindi Cai, Shiyong Zheng, Yonglang Guo\*

College of Chemistry and Chemical Engineering, Fuzhou University, Fuzhou 350108, PR China

### ARTICLE INFO

#### Article history:

Received 14 January 2012

Received in revised form 29 February 2012

Accepted 1 March 2012

Available online 10 March 2012

#### Keywords:

Carbon nanotube  
Hierarchical structure  
Methanol oxidation  
Platinum  
Trimetallic catalyst

### ABSTRACT

This work presents a general strategy to fabricate a new type of hierarchically structured trimetallic nano-catalyst. Cu nanoparticles are partially displaced by Pt<sup>4+</sup> and then further decorated by Pb (II) species on the carbon nanotube surface. The X-ray photoelectron spectroscopy and cyclic voltammograms data demonstrate that Cu is inside the particles while Pb (II) species are outside. The novel Pb–PtCu/CNT catalyst exhibits superior stability and CO poisoning tolerance during potential cycling. Methanol oxidation peak current of this novel catalyst (94.4 mA cm<sup>-2</sup>) is almost two times higher than that of the commercial PtRu/C (50 mA cm<sup>-2</sup>).

© 2012 Elsevier B.V. All rights reserved.

## 1. Introduction

One of the major issues preventing the large-scale commercialization of direct methanol fuel cell (DMFC) is the poor methanol electro-oxidation kinetics at anode electro-catalysts. The low tolerance to CO poisoning and limited active sites on a Pt catalyst, especially when the latter has limited stepped surfaces and kink sites, are the main causes [1]. Therefore, on one hand considerable efforts have been devoted to the design and synthesis of Pt-based alloy catalysts in order to promote the electro-catalytic activity through a bifunctional mechanism and/or an electronic effect [2]. On the other hand, a deliberate modification on the Pt catalyst surface with foreign atoms is conducted, which can lead to a distinct increase in catalytic activity, as shown by the enhanced methanol oxidation on the Ru- and Sn-decorated Pt nanoparticles [3]. Besides, a substantial increase in the number of Pt active sites can be achieved by dispersing Pt atoms on the surface of particles [4,5]. So far, most of the research work is just focused on one of the promoting effects. But the catalytic activity can be greatly promoted by the joint action of more than one factor above. For example, the modification with an active metal on the surface of particles with outer Pt-rich layers is a feasible way to obtain high-performance catalysts.

Pb, Bi and Sb in Pt-based catalysts have the promoting effects on the oxidation of some organic small molecules such as methanol

and formic acid on account of the modified surface geometry and chemistry [6]. Recently, the addition of Cu in Pt-based catalysts is found to be effective for enhancing the methanol electro-oxidation in acid medium [7,8]. In addition, Pt atoms can be aggregated readily on the particles surface through galvanic displacement of Pt<sup>4+</sup> to Pt by oxidizing Cu [9]. In this study, Cu particles were partially displaced by Pt<sup>4+</sup> and further decorated by Pb (II) species on the carbon nanotube (CNT) supporter for fabricating a novel Pb–PtCu/CNT catalyst, which is expected to distinctly promote the catalytic activity for methanol electro-oxidation so as to boost the commercialization of DMFC.

## 2. Experimental

### 2.1. Synthesis of catalysts

Multi-walled CNT from Shenzhen Nanotechnologies Co. Ltd. (China) was pretreated with a mixed solution of concentrated HNO<sub>3</sub>/H<sub>2</sub>SO<sub>4</sub> (1:3) at 120 °C for 2 h. Afterwards the mixture was neutralized, filtered, washed and dried overnight. The PtCu/CNT catalyst with a initial atomic ratio of 1:8 (Pt:Cu) was prepared as follows: certain amounts of CuSO<sub>4</sub> and functionalized CNT were dispersed in a mixture of water/citric acid (50/5, mass ratio) under ultrasonic stirring. A solution of NaBH<sub>4</sub> was added to reduce Cu<sup>2+</sup> ions to Cu. After this, a specific amount of H<sub>2</sub>PtCl<sub>6</sub> was dissolved in the mixture. The galvanic displacement reaction of Pt<sup>4+</sup> to Pt by oxidizing Cu was conducted for 4 h under stirring. Finally, the mixture was filtered, washed and dried overnight. For the Pb–PtCu/CNT catalyst preparation, a specific amount of PtCu/CNT was mixed

\* Corresponding author. Tel.: +86 591 8807 3608; fax: +86 591 8807 3608.  
E-mail address: [yguo@fzu.edu.cn](mailto:yguo@fzu.edu.cn) (Y. Guo).

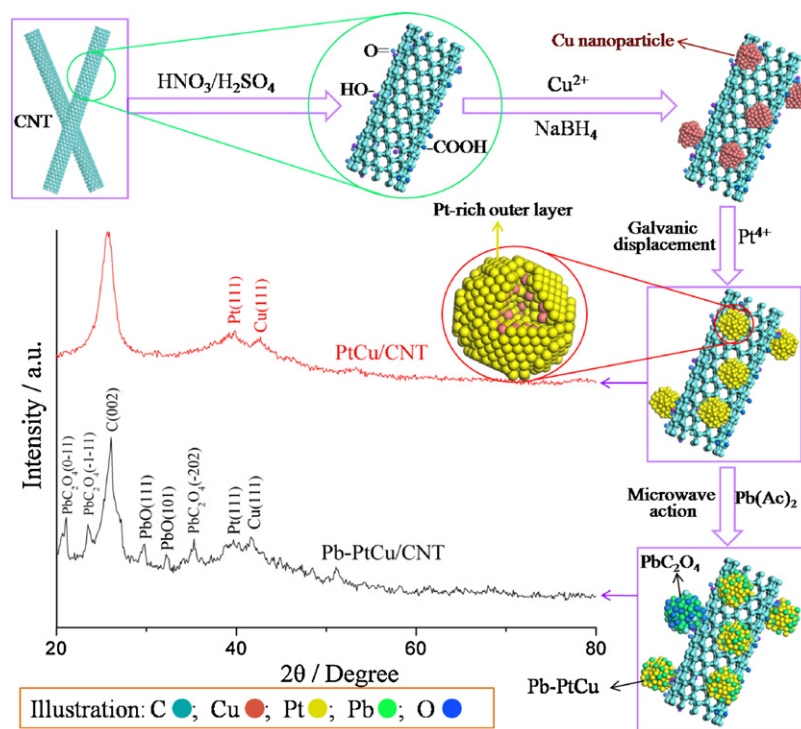


Fig. 1. Schematic drawing for the overall synthesis processes and XRD patterns of the PtCu/CNT and Pb–PtCu/CNT catalysts.

with  $\text{Pb}(\text{Ac})_2$ , KOH and HCHO in 50 ml ethylene glycol (EG) under ultrasonic stirring. The initial atomic ratio of Pt to Pb was 1:2. The mixture was treated for 5 min under a microwave power of 800 W. After cooling, the resultant suspension was filtered, washed and dried overnight. The Pt/C catalyst was prepared via a microwave approach for comparison.

## 2.2. Physical and electrochemical characterization

The Pt loadings and atomic ratios of Pb–PtCu/CNT and PtCu/CNT were determined by atomic adsorption spectroscopy (AAS, Spectr AA-220). The X-ray diffraction (XRD) patterns were carried out with a Philip X'Pert Pro MPP X-ray powder diffractometer using a Cu  $K\alpha$  radiation ( $\lambda = 1.5418 \text{ \AA}$ ) at a scan size of  $0.01289^\circ$  with a time of 49.07 s. The chemical valences of metals in the catalyst were analyzed by X-ray photoelectron spectroscopy (XPS, VG ESCALAB 250) with an Al  $K\alpha$  X-ray source of 1486.6 eV.

The electrochemical measurements were obtained using a CHI660C electrochemical working station (CH Instrument Inc.). A Pt foil and a mercury sulfate electrode (MMS) were used as the counter and reference electrodes (0.680 V versus SHE) [10], respectively. A piece of glassy carbon ( $0.1256 \text{ cm}^2$ ) covered by the catalyst was used as the working electrode. For the catalytic electrode preparation, a specific amount of the catalyst was dispersed in a suspension of 985  $\mu\text{l}$  isopropyl alcohol and 15  $\mu\text{l}$  of a 15 wt% Nafion solution (DuPont, USA) under ultrasonic stirring. An 8  $\mu\text{l}$  aliquot of the slurry was spread on the polished working electrode surface and dried at  $80^\circ\text{C}$  for 30 min. The total Pt loading on the electrode kept 4  $\mu\text{g}$ . The electrolyte was first de-aerated with high purity  $\text{N}_2$  before the measurements at  $30^\circ\text{C}$ .

## 3. Results and discussion

The practical Pt loadings of the as-prepared catalysts were 12.5 wt% for PtCu/CNT with a atomic ratio of 1:0.57 (Pt:Cu) and 8.6 wt% for Pb–PtCu/CNT with a atomic ratio of 1:2.09:0.63

(Pt:Pb:Cu), respectively. The incomplete reduction of  $\text{Cu}^{2+}$  in acid medium and the subsequent partial oxidation of Cu nanoparticles by  $\text{Pt}^{4+}$  may be the main causes for the difference between the initial and final atomic ratios.

The schematic drawing for fabricating processes of PtCu/CNT and Pb–PtCu/CNT, and the corresponding XRD patterns is shown in Fig. 1. A treatment with concentrated  $\text{HNO}_3/\text{H}_2\text{SO}_4$  was carried out on pristine CNT to produce some oxygen-containing groups of carboxyl, carbonyl and hydroxyl on its surface [11].  $\text{Cu}^{2+}$  was reduced by  $\text{NaBH}_4$  and then Cu was displaced galvanically by  $\text{Pt}^{4+}$  [12]. The interaction between Pt and Cu is shown by the slightly positive shift of Pt (1 1 1) peak from  $39.7^\circ$  to  $40.0^\circ$  and the negative shift of Cu (1 1 1) peak from  $43.3^\circ$  to  $42.8^\circ$  compared to the pure Pt and Cu (JCPDS-ICDD Nos. 65–2868 & 04–0836) in the XRD patterns, respectively. Pb was precipitated in the form of Pb oxides in the microwave action, as shown by the XRD pattern of Pb–PtCu/CNT. Meanwhile, several small peaks assigned to the formation of  $\text{PbC}_2\text{O}_4$  are found, which is caused by the combination of  $\text{Pb}^{2+}$  and  $\text{C}_2\text{O}_4^{2-}$  ions deriving from EG oxidation by the microwave radiation [13].

A XPS analysis was used to characterize the valence states of metals in the Pb–PtCu/CNT catalyst, as shown in Fig. 2. The Pt 4f region demonstrates two pairs of asymmetric peaks (Fig. 2A), indicating the different oxidation states of Pt. The intense doublet peak belongs to Pt (0) and the weak one is assigned to Pt (II) species, such as PtO and  $\text{Pt}(\text{OH})_2$  [14]. The Pb 4f signal in Fig. 2B is almost produced by Pb (II) species, indicating that most Pb atoms were not alloyed with Pt and Cu in the microwave action. Therefore, these Pb (II) species may exist on the surface of PtCu nanoparticles and/or CNT. The Cu 2p signal (Fig. 2C) is weak, resulting from two factors: the first is that the Cu content in the catalyst is lower than the Pt or Pb content; the second may be that Cu atoms are inside the particles, which makes its signal weaker in the XPS test [15].

The electrochemical measurement data are shown in Fig. 3. PtCu/CNT presents a larger active area of hydrogen adsorption–desorption (Fig. 3A), similar to the result in the literature [16]. The broad featureless shoulder region from  $-0.55$  to

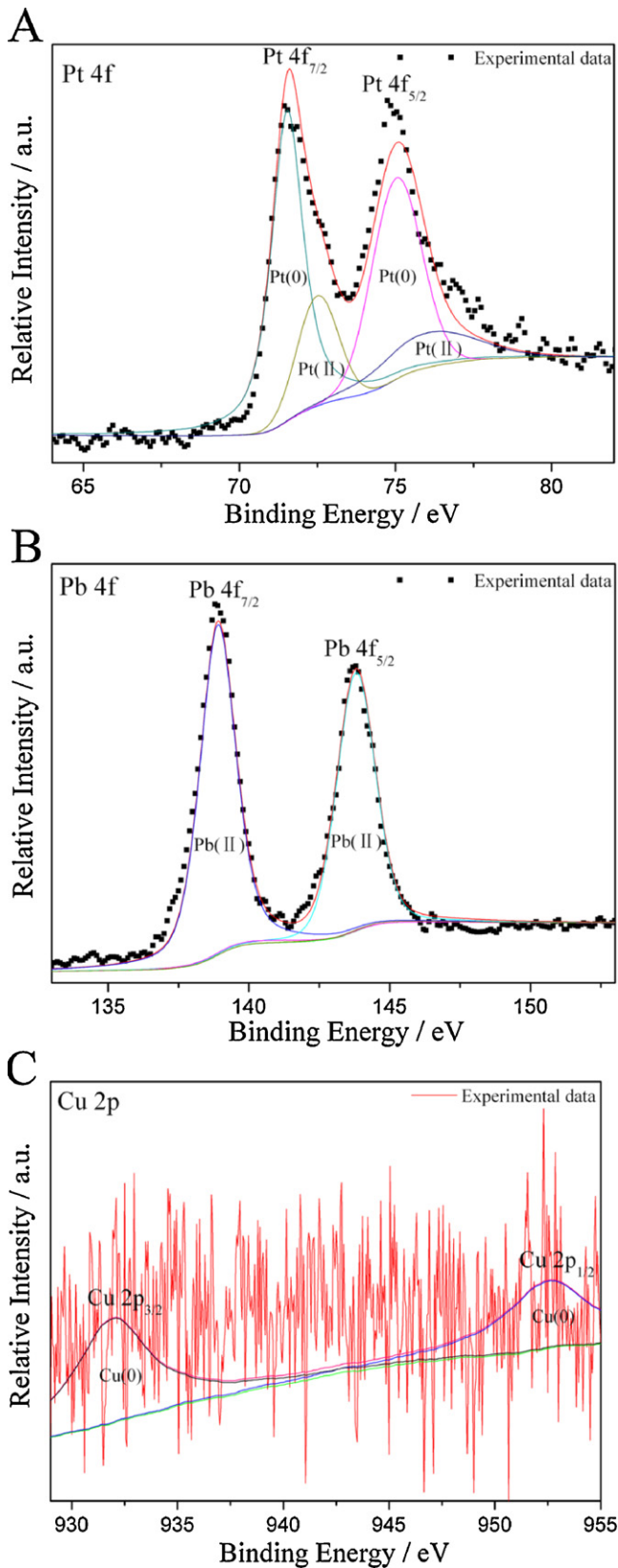


Fig. 2. XPS spectra of Pb–PtCu/CNT: (A) Pt 4f, (B) Pb 4f and (C) Cu 2p regions.

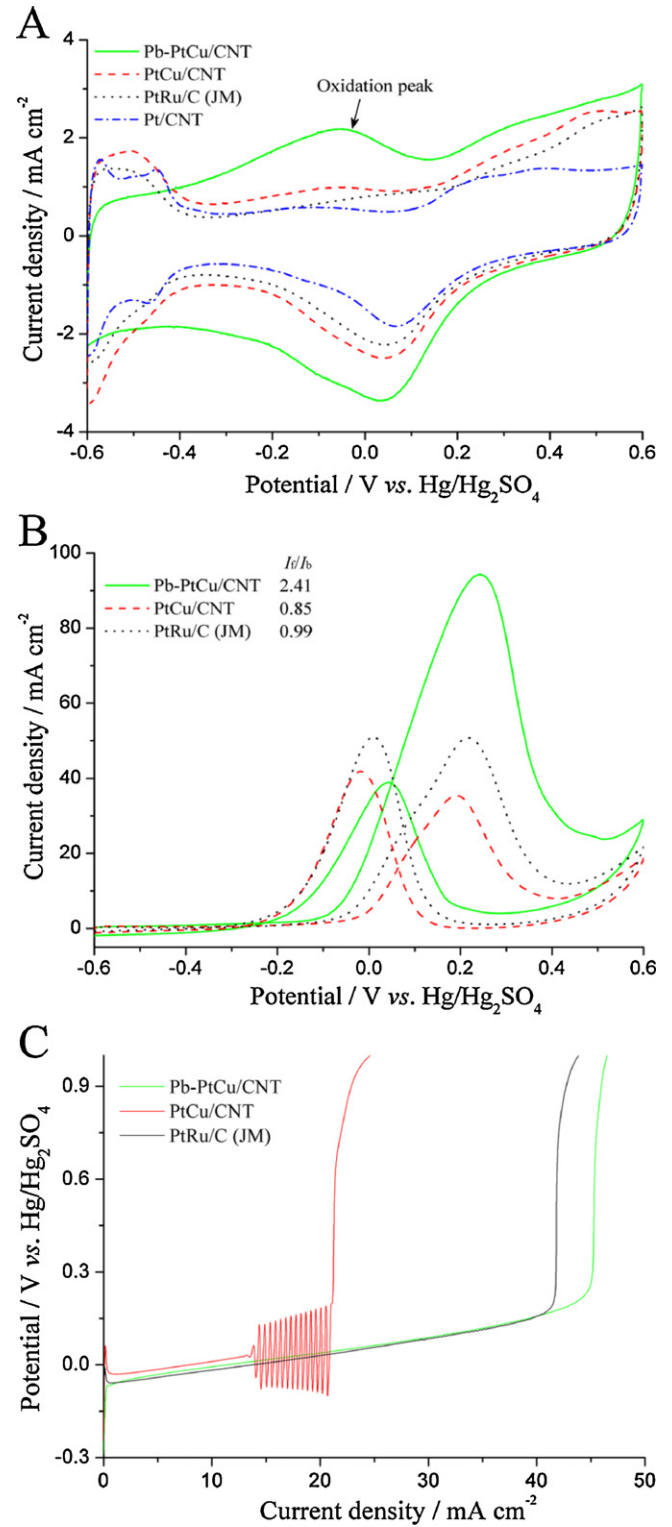
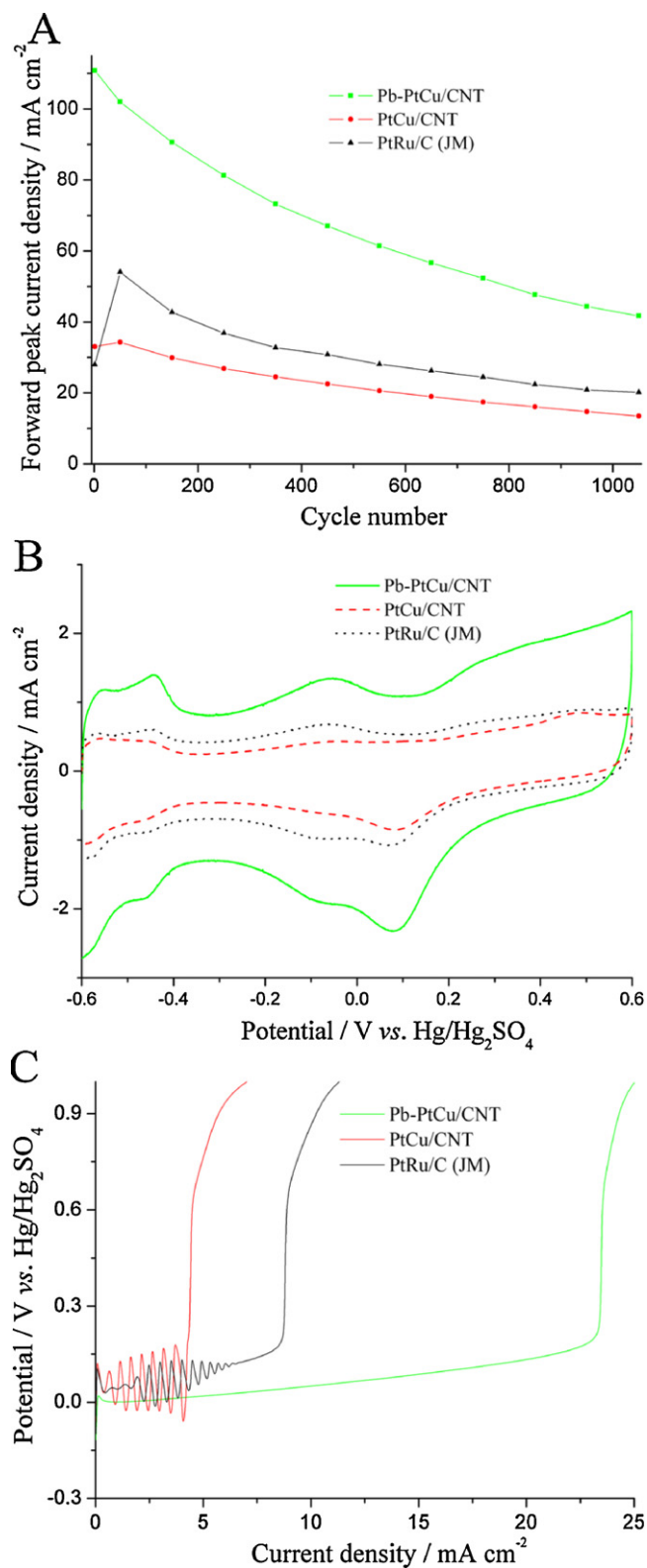


Fig. 3. Cyclic voltammograms of the catalysts in (A) 0.5 M H<sub>2</sub>SO<sub>4</sub> and (B) 0.5 M H<sub>2</sub>SO<sub>4</sub> + 1 M CH<sub>3</sub>OH at 50 mV s<sup>-1</sup>. (C) Linear current sweep of the catalysts for methanol oxidation at a scan rate of 0.16 mA cm<sup>-2</sup> s<sup>-1</sup>.

–0.4 V develops on PtCu/CNT, possibly due to the contribution of stepped surfaces and kink sites [12]. No anodic currents caused by the dissolution of Cu from the lattice are observed, suggesting that Cu was inside the particles and Pt atoms comprised the outer layers. The deposition of Pb (II) species results in a decrease in



**Fig. 4.** (A) The evolution of forward peak current densities ( $I_f$ ) of the catalysts in 1050 cycles. (B) Cyclic voltammograms in 0.5 M  $\text{H}_2\text{SO}_4$  and (C) Linear current sweep after 1050 cycles. Solution: 0.5 M  $\text{H}_2\text{SO}_4$  + 1 M  $\text{CH}_3\text{OH}$ .

the hydrogen adsorption–desorption area, indicating that Pb (II) species covered the partial surface of PtCu particles. Meanwhile, the oxidation peak in Pb–PtCu/CNT was greatly enhanced. This is critical to the electro-catalytic oxidation of methanol because it facilitates the removal of CO-like species [17]. Methanol oxidation reaction (Fig. 3B) on the Pb–PtCu/CNT catalyst exhibits not only the highest specific activity ( $94.4 \text{ mA cm}^{-2}$ ), approximately two times the value of commercial PtRu/C ( $50.0 \text{ mA cm}^{-2}$ ), but also the highest ratio of forward to backward peak current densities ( $I_f/I_b$ ) (2.41). The  $I_f/I_b$  ratio signifies the electro-oxidation ability toward residual intermediate species formed during methanol oxidation [18]. The anti-poisoning abilities of the catalysts were further evaluated by linear current sweep curves, as shown in Fig. 3C. A potential oscillation is observed on PtCu/CNT due to the poisoning by CO formed in methanol dehydrogenation processes [19]. Pb–PtCu/CNT shows the highest current density of  $45.0 \text{ mA cm}^{-2}$  at the point of steep hop in potential.

Long-term potential cycling was used to estimate the stabilities of the catalysts. It is obvious that the Pb–PtCu/CNT catalyst keeps the best catalytic activity in the cycles (Fig. 4A). After 1050 cycles, the hydrogen adsorption–desorption peaks of PtCu/CNT and commercial PtRu/C decrease greatly while they increase obviously on Pb–PtCu/CNT and their profiles become more apparent (Fig. 4B) due to the partial dissolution of Pb from PtCu particles surface. The potential oscillation of PtRu/C reveals the dissolution of Ru in the potential cycles (Fig. 4C) [19]. The Pb–PtCu/CNT catalyst exhibits the best stability and tolerance toward CO poisoning before and after cycling.

#### 4. Conclusions

The novel synthesized Pb–PtCu/CNT catalyst has two characteristics: the hierarchical structure with outer Pt-rich layers and modification with foreign atoms. It exhibits rather high catalytic activity toward methanol oxidation, quite better stability and high CO poisoning tolerance. The outstanding performance of the Pb–PtCu/CNT catalyst makes it an excellent potential candidate for the application in DMFC.

#### Acknowledgment

This work was financially supported by the National Natural Science Foundation of China (No. 51072037).

#### References

- [1] N. Tian, Z.Y. Zhou, S.G. Sun, Y. Ding, Z.L. Wang, *Science* 316 (2007) 732–735.
- [2] J. Luo, P.N. Njoki, Y. Lin, D. Mott, L.Y. Wang, C.J. Zhong, *Langmuir* 22 (2006) 2892–2898.
- [3] J.P. MacDonald, B. Gaultieri, N. Runga, E. Teliz, C.F. Zinola, *Int. J. Hydrogen Energy* 33 (2008) 7048–7061.
- [4] Y.Y. Xu, Y.N. Dong, J. Shi, M.L. Xu, Z.F. Zhang, X.K. Yang, *Catal. Commun.* 13 (2011) 54–58.
- [5] P. Ochal, J.L.G. de la Fuente, M. Tsyppkin, F. Seland, S. Sunde, N. Muthuswamy, M. Rønning, D. Chen, S. Garcia, S. Alayoglu, B. Eichhorn, *J. Electroanal. Chem.* 655 (2011) 140–146.
- [6] E. Casado-Rivera, D.J. Volpe, L. Alden, C. Lind, C. Downie, T. Vázquez-Alvarez, A.C.D. Angelo, F.J. DiSalvo, H.D. Abruña, *J. Am. Chem. Soc.* 126 (2004) 4043–4049.
- [7] S. Papadimitriou, S. Armanyanov, E. Valova, A. Hubin, O. Steenhaut, E. Pavlidou, G. Kokkinidis, S. Sotiropoulos, *J. Phys. Chem. C* 114 (2010) 5217–5223.
- [8] M.K. Jeon, J.S. Cooper, P.J. McGinn, *J. Power Sources* 185 (2008) 913–916.
- [9] Z.D. Wei, Y.C. Feng, L. Li, M.J. Liao, Y. Fu, C.X. Sun, Z.G. Shao, P.K. Shen, *J. Power Sources* 180 (2008) 84–91.
- [10] M.H. Huang, L.R. Li, Y.L. Guo, *Electrochim. Acta* 54 (2009) 3303–3308.
- [11] V. Datsyuk, M. Kalyva, K. Papagelis, J. Parthenios, D. Tasis, A. Siokou, I. Kallitsis, C. Galiotis, *Carbon* 46 (2008) 833–840.
- [12] A. Sarkar, A. Manthiram, *J. Phys. Chem. C* 114 (2010) 4725–4732.
- [13] M. Gürü, A.Y. Bilgesü, V. Pamuk, *Bioresour. Technol.* 77 (2001) 81–86.
- [14] T.Y. Jeon, S.J. Yoo, Y.H. Cho, S.H. Kang, Y.E. Sung, *Electrochem. Commun.* 12 (2010) 1796–1799.

- [15] A. Virnovskaia, S. Jørgensen, J. Hafizovic, Ø. Prytz, E. Kleimenov, M. Hävecker, H. Bluhm, A. Knop-Gericke, R. Schlögl, U. Olsbye, *Surf. Sci.* 601 (2007) 30–43.
- [16] H. Zhu, X.W. Li, F.H. Wang, *Int. J. Hydrogen Energy* 36 (2011) 9151–9154.
- [17] M. Futamata, L.Q. Luo, *J. Power Sources* 164 (2007) 532–537.
- [18] Z.L. Liu, X.Y. Ling, X.D. Su, J.Y. Lee, *J. Phys. Chem. B* 108 (2004) 8234–8240.
- [19] Z.Z. Zhao, X. Fang, Y.L. Li, Y. Wang, P.K. Shen, F.Y. Xie, X. Zhang, *Electrochem. Commun.* 11 (2009) 290–293.